ЖУРНАЛ ФІЗИЧНИХ ДОСЛІДЖЕНЬ
т. 22, № 1 (2018) 1701(9 с.)

JOURNAL OF PHYSICAL STUDIES
v. 22, No. 1 (2018) 1701(9 p.)

ANISOTROPIC WURTZITE RESONANCE TUNNELING STRUCTURES: STATIONARY SPECTRUM OF ELECTRON AND OSCILLATOR STRENGTHS OF QUANTUM TRANSITIONS

I. V. Boyko
Ternopil Ivan Puluj National Technical University
56, Ruska St., Ternopil, 46001, Ukraine
e-mail: boyko.i.v.theory@gmail.com
(Received January 14, 2018; in final form — February 21, 2018)

Within the dielectric continuum model and the model of effective masses for the electron, self-consistent solutions to the Schrödinger–Poisson system of equations taking into account the contribution of piezoelectric and spontaneous polarizations were found.

The theory of stationary electronic states, taking into account the internal fields caused by piezoelectric and spontaneous polarizations occurring in the nanostructure was developed for the three-barrier wurtzite anisotropic resonance-tunneling structure with binary and ternary components.

For nanostructure, which functioned as a cascade of experimentally realized quantum cascade detector, the calculation of the potential profile, stationary electron energy spectrum and oscillator strengths of quantum transitions was carried out. The geometric configurations of the nanostructure, for which the intensity of the detector quantum transitions between the working energetic states is the largest, were established.

Key words: quantum cascade detector, resonance tunnelling structure, piezoelectric polarization, spontaneous polarization, oscillator strengths.

DOI: https://doi.org/10.30970/jps.22.1701

PACS number(s): 73.21.Ac, 78.20.hb, 78.67.−n

I. INTRODUCTION

In the modern physics of semiconductors, considerable attention is paid to the study of the properties of low-dimensional 3D nanosystems — resonance-tunnel structures (RTS). In recent years, on the basis of binary and triple compounds of nitrides InN, GaN, AlN, quantum cascade lasers (QCL) [1,2] and detectors (QCD) [3–5] operating in the infrared range of electromagnetic waves were created. Compared to the QCL [6, 7] and the QCD [8, 9], which are based on binary and triple arsenide semiconductor GaAs, InAs, AlAs, etc., the mentioned nanodevices have a number of functional advantages. In particular, the temperature stability of nitrides allows nanodevices to operate in a range from cryogenic to room temperature. At the same time, their considerable optical activity is ensured.

Group III-nitrides have a strong interatomic bond and a large band gap, their crystalline lattice has a hexagonal structure of wurtzite, which determines the anisotropy of the physical properties of such materials. This determines the significant differences in the calculation of potential RTS profiles, the electron energy spectrum, and the phonon spectrum in comparison with isotropic systems having a cubic structure of a crystalline lattice.

The calculation of the potential profiles of anisotropic RTS is a problem not solved to the end. The theory of internal fields arising in nanostructures with a small number of layers, which was developed in the papers [10–15], cannot be directly applied to a multilayer RTS. At the same time, there are currently only two approaches to calculating potential RTS profiles, each of which has its own significant shortcomings. The first approach proposed in [16–18] is rather rough, since it allows only the contribution of internal fields to be taken into account in the value of an effective potential profile. The second approach, proposed in many papers [19–23], is based on the numerical simulation of solutions of a self-consistent system of the Schrödinger and Poisson equations. For example, in work [19], the boundary conditions for the electron wave function at the boundaries of the nanosystem are not used. The main disadvantage of this approach is that it is often not universal and cannot be applied to calculations of the potential profiles of various RTS. It can also be implemented mainly on powerful computers.

In the proposed work, a consistent theory of stationary electronic states and oscillator strengths of quantum transitions is developed for the anisotropic two-well RTS AlN/GaN/AlN/$Al_xGa_{1-x}N$/AlN of wurtzite type, which is a separate cascade of experimentally created QCD operating in the infrared range of electromagnetic waves [5]. To do this, by finding the solution to the system of the self-consistent Schrödinger and Poisson equations, the calculation of the potential RTS profile was performed. The calculation of the energy spectrum of the electron and the oscillator strengths of quantum transitions depending on the geometric parameters of the investigated RTS was performed for the first time.

II. THE EFFECTIVE POTENTIAL OF A NANOSTRUCTURE. THE SELF-CONSISTENT SCHRÖDINGER AND POISSON SYSTEM OF EQUATIONS

A two-well RTS, which is located so that in the Cartesian coordinate system the OZ axis is perpendicular to the boundaries of the separation of the nanostructure layers, is considered (Fig. 1). The media (0), (1), (3), (5), (6) are assumed to correspond to the semiconductor material AlN, medium (2) — GaN, medium (4) — $Al_{0.58}Ga_{0.42}N$.

Using the model of effective masses for an electron we have:

$$m(z) = m_0 \left\{ \theta(-z) + \theta(z - z_5) + \sum_{p=0}^{2} [\theta(z - z_{2p}) - \theta(z - z_{2p+1})] \right\} + m_1[\theta(z - z_1) + \theta(z - z_2)] + m_2[\theta(z - z_3) + \theta(z - z_4)], \tag{1}$$

where $\theta(z)$ is the Heaviside step function, $z_{-1} \to -\infty$, $z_6 \to \infty$, $m_0 = m^{(0)} = m^{(1)} = = m^{(3)} = m^{(5)} = m^{(6)}$, $m_1 = m^{(2)}$ and $m_2 = m^{(4)}$ are effective electron masses in the potential barriers and wells of RTS, respectively.

Similarly, for the dielectric permeability of RTS we have:

$$\varepsilon(z) = \varepsilon^{(0)} \left\{ \theta(-z) + \theta(z - z_5) + \sum_{p=0}^{2} [\theta(z - z_{2p}) - \theta(z - z_{2p+1})] \right\} + \varepsilon^{(1)}[\theta(z - z_1) + \theta(z - z_2)] + \varepsilon^{(2)}[\theta(z - z_3) + \theta(z - z_4)], \tag{2}$$

$\varepsilon^{(0)} = \varepsilon^{(1)} = \varepsilon^{(3)} = \varepsilon^{(5)} = \varepsilon^{(6)}$, $\varepsilon_1 = \varepsilon^{(2)}$ and $\varepsilon_2 = \varepsilon^{(4)}$ are the dielectric permeabilities of the RTS layers material, respectively.

The effective potential of the RTS for electron is found as follows:

$$V(z) = \Delta E_{\mathrm{C}}(z) + V_{\mathrm{H}}(z) + V_{\mathrm{HL}}(z) + V_{\mathrm{E}}(z) \tag{3}$$

where the definition of its components $\Delta E_{\mathrm{C}}(z)$, $V_{\mathrm{H}}(z)$, $V_{\mathrm{HL}}(z)$, $V_{\mathrm{E}}(z)$ will be established below.

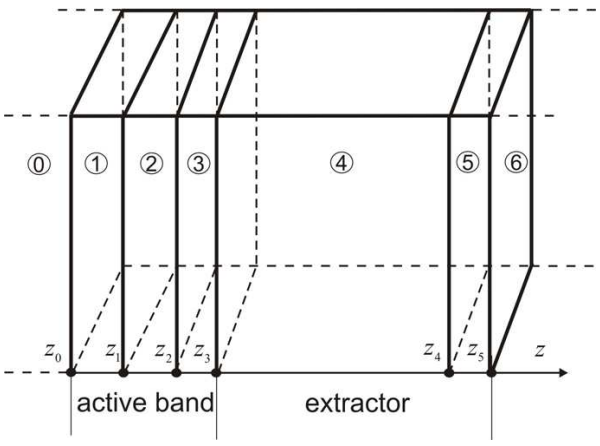

Fig. 1. Geometric scheme of nanostructure.

The energy spectrum of an electron E_n and its wave functions $\Psi(z)$ are determined by the solutions of the self-consistent system of the Schrödinger and Poisson equations:

$$\begin{cases} -\dfrac{\hbar^2}{2}\dfrac{d}{dz}\left(\dfrac{1}{m(z)}\dfrac{d\Psi(z)}{dz}\right) + V(z)\Psi(z) = E\Psi(z), \\ \dfrac{d}{dz}\left(\varepsilon(z)\dfrac{dV_{\mathrm{H}}(z)}{dz}\right) = -e\rho(z), \end{cases} \tag{4}$$

where $\rho(z)$ is the free charge density inside the nanosystem, and $V_{\mathrm{H}}(z)$ is the potential determined by the contribution of these charges.

On the boundaries of the RTS layers the conditions of the continuity of the wave function $\Psi(z)$ and the flows of its probabilities are fulfilled:

$$\Psi^{(p)}(z_p) = \Psi^{(p+1)}(z_p); \qquad \left.\frac{d\Psi_n^{(p)}(z)}{m(z)dz}\right|_{z=z_p-\varepsilon} = \left.\frac{d\Psi_n^{(p+1)}(z)}{m(z)dz}\right|_{z=z_p+\varepsilon}. \tag{5}$$

Similarly, on the RTS heteroboundaries we have conditions for the continuity of the potential $V_{\mathrm{H}}(z)$ and the vector of electric displacement field:

$$V_{\mathrm{H}}^{(p)}(z_p) = V_{\mathrm{H}}^{(p+1)}(z_p); \qquad \left.\frac{\varepsilon^{(p)}d\varphi_{\mathrm{H}}^{(p)}(z)}{dz}\right|_{z=z_p\varepsilon} - \left.\frac{\varepsilon^{(p+1)}d\varphi_{\mathrm{H}}^{(p+1)}(z)}{dz}\right|_{z=z_p+\varepsilon} = -\sigma(z_p), \tag{6}$$

where in (5) and (6) $\varepsilon \to +0$; $p = 0 \div 5$, and the second condition in expression (6) takes into account the pres-

ence of surface charges on the nanosystem heteroboundaries, which are the result of the different magnitude of the total polarization in the adjacent RTS layers. For the potential $V_{\rm H}(z)$ outside the RTS, the conditions for its disappearance are fulfilled:

$$V_{\rm H}(z)|_{z\to 0} \to 0;\ V_{\rm H}(z)|_{z\to z_5} \to 0. \tag{7}$$

In Eq. (3),

$$\Delta E_C(z) = \begin{cases} 0.765(E_g({\rm AlN}) - E_g({\rm GaN})),\ z<0,\ 0\le z<z_1,\ z_2\le z<z_3, z_4\le z<z_5,\ z>z_5; \\ 0,\ z_1\le z<z_2; \\ 0.765(E_g({\rm Al}_{0.58}{\rm Ga}_{0.42}{\rm N}) - E_g({\rm GaN})),\ \ z_3\le z<z_4 \end{cases} \tag{8}$$

is a potential RTS profile for the electron calculated without taking into account the electric field of piezoelectric and spontaneous polarizations. The dependence of the bandgap on the temperature T in (8) for a ${\rm Al}_x{\rm Ga}_{1-x}{\rm N}$ semiconductor is given by the Varshni relation [24, 25]:

$$E_g(x,T) = E_g(x,0) - \frac{a(x)T^2}{T+b(x)} \tag{9}$$

being in dependence on the value of x:

$$E_g(x,0) = xE_g({\rm AlN}) + (1-x)E_g({\rm GaN}) + \alpha x(1-x), \tag{10}$$

$E_g({\rm AlN}) = 6.25$ eV and $E_g({\rm GaN}) = 3.51$ eV are the bandgap energies for AlN and GaN respectively, $\alpha = 0.7$ eV is a bowing parameter, $a(x) = (1.799x + 0.909(1-x)) \times 10^{-3}$ (eV/K) and $b(x) = 1462x + 830(1-x)$ (K) are the Varshni parameters.

Besides, in (3):

$$V_{\rm HL}(z) = -\left(\frac{9}{4\pi^2}\right)^{1/3}\left[1 + \frac{0.6213 r_s}{21}\ln\left(1+\frac{21}{r_s(z)}\right)\right] \times \frac{e^2}{4\pi\varepsilon_0 r_s(z)\varepsilon(z)a^*_{\rm B}(z)} \tag{11}$$

is the exchange-correlation potential calculated in the Hedin–Lundquist approximation [26], where $r_s(z) = \left(\frac{4\pi}{3}a^{*3}_{\rm B}n(z)\right)^{-1/3}$ is a dimensionless function that characterizes the electron gas in the RTS, in relation to the effective Bohr radius $a^*_{\rm B}(z) = \varepsilon(z)/m(z)a_{\rm B}$, $a_{\rm B}$ is the Bohr radius, $n(z)$ is the concentration of carriers creating a static spatial charge.

The potential energy $V_{\rm E}(z)$, which specifies the contribution of the interaction of an electron with the internal fields of the spontaneous and piezoelectric polarizations, is found by the expression:

$$V_{\rm E}(z) = \begin{cases} 0, & z<0, \\ eF_1 z, & 0\le z<z_1, \\ eF_1 z_1 - eF_2 z, & z_1\le z<z_2, \\ -eF_2 z_2 + eF_3 z, & z_2\le z<z_3, \\ eF_3 z_3 - eF_4 z, & z_3\le z<z_4, \\ -eF_4 z_4 + eF_5 z, & z_4\le z<z_5, \\ 0, & z\ge z_5 \end{cases} \tag{12}$$

where F_p, $p = 1\ldots 5$, are the values of the internal electric fields magnitudes appearing in the RTS.

III. CALCULATION OF THE INTERNAL ELECTRIC FIELDS MAGNITUDES IN THE NANOSTRUCTURE

The value of the macroscopic polarization $P^{(p)}$ in an arbitrary p-th RTS layer is the sum of the spontaneous $P^{(p)}_{\rm SP}$ and piezoelectric $P^{(p)}_{\rm PZ}$ polarizations:

$$P^{(p)} = P^{(p)}_{\rm SP} + P^{(p){\rm SP}}_{\rm PZ}. \tag{13}$$

Piezoelectric polarization for a three-component semiconductor layer of $A_xB_{1-x}N$-type depending on the concentration x of the component A is determined in the linear approximation:

$$P^{(p)}_{\rm PZ(SP)}(x) = P^{AN(p)}_{\rm PZ(SP)}(\eta^{(p)}(x)) + (1-x)P^{BN(p)}_{\rm PZ(SP)}(\eta^{(p)}(x)) \tag{14}$$

In expression (13) the values $P^{AN(p)}_{\rm PZ(SP)}(\eta^{(p)}(x))$ and $P^{BN(p)}_{\rm PZ(SP)}(\eta^{(p)}(x))$ — due to the inconsistency of the lattice constants of the RTS layers — depend on the magnitude of the basal deformation $\eta^{(p)} = \eta^{(p)}(x) = (a_{\rm subs} - a(x))/a(x)$, where $a(x)$ and $a_{\rm subs}$ are lattice constants of the RTS and substrate material layers respectively [27]:

$$\begin{aligned} a(x) &= 0.31986 - 0.00891x, \\ a_{\rm buf} &= \sum_{p=1}^{5} A^{(p)}\frac{d_p}{a^{(p)}}\Big/\sum_{k=1}^{5}\frac{d_p}{(a^{(p)})^2}; \\ A^{(p)} &= C^{(p)}_{11} + C^{(p)}_{12} - 2\frac{(C^{(p)}_{13})^2}{C^{(p)}_{33}}, \end{aligned} \tag{15}$$

where a^p is the material lattice constant, d_p is thickness, $C^{(p)}_{11}$, $C^{(p)}_{12}$, $C^{(p)}_{13}$, $C^{(p)}_{33}$ are elastic constants of the RTS p-th layer.

The value of the piezoelectric polarization for an arbitrary layer of the RTS is defined as:

$$
\begin{aligned}
P_{\mathrm{PZ}}^{(p)} &= 2\eta^{(p)}\, e_{31}^{(p)} + \eta_z^{(p)} e_{33}^{(p)} \\
&= 2\eta^{(p)}\, e_{31}^{(p)} + \left(-\frac{2C_{13}^{(p)}}{C_{33}^{(p)}} \eta^{(p)} \right) e_{33}^{(p)} \\
&= 2\eta^{(p)} \left(e_{31}^{(p)} - e_{33}^{(p)} \frac{C_{13}^{(p)}}{C_{13}^{(p)}} \right), \\
\eta_z^{(p)} &= -\frac{2C_{13}^{(p)}}{C_{33}^{(p)}} \eta^{(p)},
\end{aligned}
\tag{16}
$$

where $e_{31}^{(p)},\ e_{33}^{(p)}$ are piezoelectric constants.

The values of internal electric fields F_p are determined from the continuity condition of the electrical displacement vector $\bar{D}_p = \varepsilon^{(p)} \bar{F}_p + \bar{P}_p$ on all the RTS heteroboundaries, that is:

$$
\bar{D}_p = \bar{D}_{p+1}. \tag{17}
$$

Besides, the condition is provided, that the total potential drop across the RTS is zero is satisfied [12, 16]:

$$
\sum_{p=1}^{5} F_p d_p = 0. \tag{18}
$$

From the relations (17) and (18) an expression for the electric field in an arbitrary layer of the RTS is found:

$$
F_p = \sum_{k=1;\ k\neq p}^{5} (P_k - P_p) \frac{d_k}{\varepsilon^{(k)}} \Bigg/ \varepsilon^{(p)} \sum_{k=1}^{5} \frac{d_k}{\varepsilon^{(k)}}, \tag{19}
$$

d_k is the thickness of the k-th RTS layer.

IV. SELF-CONSISTENT SOLUTIONS TO THE SCHRÖDINGER AND POISSON SYSTEM OF EQUATIONS

Solutions to the self-consistent system of the Schrödinger and Poisson equations (4) will be found on a uniform grid [28]:

$$
\bar{\omega} = \left\{ z_s = sh,\ s = 0,\ 1,\ \ldots N,\ h = \frac{l}{N} \right\} \tag{20}
$$

where $l = d_1 + d_2 + d_3 + d_4 + d_5 = z_5$ is total RTS thickness.

Using the finite difference method [28], the first and the second derivatives are approximated as:

$$
\begin{aligned}
\left. \frac{d\Psi^{(s)}(z)}{dz} \right|_{z=z_s} &= \frac{\Psi_{s+1} - \Psi_s}{h}; \\
\left. \frac{d^2\Psi^{(s)}(z)}{dz^2} \right|_{z=z_s} &= \frac{\Psi_{s+1} - 2\Psi_s + \Psi_{s-1}}{h^2}.
\end{aligned}
\tag{21}
$$

Besides, for wave functions, the conditions of periodicity similar to the BornЦvon Karman boundary condition are fulfilled, so:

$$
\Psi_0 = \Psi_N;\ \Psi_1 = \Psi_{N+1}. \tag{22}
$$

Then the wave functions of the electron Ψ_s and the solutions to the Poisson equation φ_s taking into account the boundary conditions for them (5), (6) for the approximation of derivatives in accordance with (21), are determined by the solutions of matrix equations:

$$
\begin{gathered}
\sum_{r=1}^{N} A_{sr}\Psi_s = f_s,\ ;\ \sum_{r=1}^{N} B_{sr}\varphi_s = F_s, \\
\Psi_s = \begin{pmatrix} \Psi_1 \\ \Psi_2 \\ \Psi_3 \\ \Psi_4 \\ \Psi_s \\ \vdots \\ \Psi_N \end{pmatrix};\quad f_s = \begin{pmatrix} K_s h \\ 0 \\ 0 \\ 0 \\ 0 \\ \vdots \\ 0 \end{pmatrix};\ \varphi_s = \begin{pmatrix} \varphi_1 \\ \varphi_2 \\ \varphi_3 \\ \varphi_4 \\ \varphi_s \\ \vdots \\ \varphi_N \end{pmatrix};\ F_s = \begin{pmatrix} -\rho_1 h \\ P_2 - P_1 \\ \vdots \\ -\rho_{s-1} h \\ P_s - P_{s-1} \\ \vdots \\ -\rho_N h \\ P_{N+1} - P_N \end{pmatrix},
\end{gathered}
\tag{23}
$$

where $\varphi_0 = \varphi_{N+1} = 0$, which follows from condition (7),
$K_s = \hbar^{-1}\sqrt{2m_1(\Delta E_C(z_s) - E)}$. In expression (23) $A_{sr},\ B_{sr}$ $(s = 1 \ldots n,\ r = 1 \ldots n)$ are matrices for which elements:

$$
A_{sr} = \begin{cases} 1, & r = s-1, \\ -\left(1 + \dfrac{m_s}{m_{s+1}}\right), & r = s, \\ \dfrac{m_s}{m_{s+1}}, & r = s+1, \\ 0, & \text{otherwise} \end{cases};\quad B_{sr} = \begin{cases} \varepsilon^{(s-1)} & r = s-1, \\ -(\varepsilon^{(s-1)} + \varepsilon^{(s)}), & r = s, \\ \varepsilon^{(s)} & r = s+1, \\ 0, & \text{otherwise} \end{cases}
\tag{24}
$$

if the nodes z_s of the grid coincide with the heteroboundaries of the RTS and

$$A_{sr} = \begin{cases} 1, & r = s-1, \\ (k_s^2 - \chi_s^2)h^2 - 2, & r = s, \\ -1, & r = s+1, \\ 0, & \text{otherwise} \end{cases}; \qquad B_{sr} = \begin{cases} \varepsilon^{(s)}, & r = s-1, \\ -(\varepsilon^{(s)} + \varepsilon^{(s+1)}), & r = s, \\ \varepsilon^{(s+1)}, & r = s+1, \\ 0, & \text{otherwise} \end{cases} \tag{25}$$

otherwise.

In expression (25):

$$k_s = \hbar^{-1}\sqrt{2m_s E};\ \chi_s = \hbar^{-1}\sqrt{2m_s V(z_s)};$$
$$m_s = \begin{cases} m_0, & \text{wells}, \\ m_1, & \text{barriers}. \end{cases}. \tag{26}$$

The stationary spectrum $E_n^{(s)}$ of electron is determined from the dispersion equation:

$$\det\left|A_{sr} - E_n^{(s)} I\right| = 0, \tag{27}$$

were $n = 1,\ 2,\ \ldots$ is the number of the energy level of the stationary electronic spectrum, I is the unit matrix of dimensions $N \times N$.

The resulting wave function of an electron in the RTS can be written as:

$$\Psi_n(E_n, z) = \sum_{p=1}^{N} \Psi_n^{(p)}(E_n, z)\left[\theta(z - z_{p-1}) - \theta(z - z_p)\right]. \tag{28}$$

Further, in the ratio (25):

$$\rho_s = \rho(z) = \sigma(z_s)\delta(z_{s+1} - z_s) + e(N_{\mathrm{D}}^+ - n(z_s)) \tag{29}$$
$$= \left(P(z)|_{z=z_s+0} - P(z)|_{z=z_s-0}\right)/h + e(N_{\mathrm{D}}^+ - n(z_s)) = (P_{s+1} - P_s)/h + e(N_{\mathrm{D}}^+ - n(z_s)),$$

where the concentration of ionized donor impurities:

$$N_{\mathrm{D}}^+ = \frac{N_{\mathrm{D}}}{1 + 2\exp\left(\dfrac{E_{\mathrm{F}} - E_n}{k_{\mathrm{B}}T}\right)} \tag{30}$$

N_{D} is the concentration of donor impurities, $\delta(z)$ is the Dirac delta function.

Concentration of electrons in the RTS:

$$n(z) = n_0(z)\sum_n \left|\Psi(E_n,\ z)\right|^2 \ln\left|1 + \exp\left(\frac{E_{\mathrm{F}} - E_n}{k_{\mathrm{B}}T}\right)\right| n_0(z) = \frac{m(z)k_{\mathrm{B}}T}{\pi\hbar^2}. \tag{31}$$

The Fermi level of the material of the RTS layers E_{F} is determined from the condition of charge neutrality of the nanostructure:

$$\int_0^l \left[n(z) - N_{\mathrm{D}}^+\right] dz = 0. \tag{32}$$

The oscillator strengths of quantum transitions using the Simpson's rule [28] are found as follows:

$$f_{m,m'} = \frac{2(E_m - E_{m'})}{\hbar^2}\sum_{p=1}^{N} m_p \left|\int_{z_{p-1}}^{z_p} z\Psi_m^{*(p)}(E_m, z)\Psi_{m'}^{(p)}(E_{m'}, z)dz\right|^2$$
$$= \frac{(E_m - E_{m'})}{3\hbar^2}\sum_{p=1}^{N} m_p \Big|z_{p-1}\Psi_m^{*(p)}(E_m, z_{p-1})\Psi_{m'}^{(p)}(E_{m'}, z_{p-1}) \tag{33}$$
$$+ 2(z_{p-1} + z_{p+1})\Psi_m^{*(p)}\left(E_m, \frac{z_{p-1} + z_{p+1}}{2}\right)\Psi_{m'}^{(p)}\left(E_{m'}, \frac{z_{p-1} + z_{p+1}}{2}\right)$$
$$+\ z_{p+1}\Psi_m^{*(p)}(E_m, z_{p+1})\Psi_{m'}^{(p)}(E_{m'}, z_{p+1})\Big|^2.$$

Now the self-consistent solution to the Schrödinger and Poisson system of equations (4) is obtained using the method of successive l iterations according to the scheme:

$$\begin{cases} -\dfrac{\hbar^2}{2}\dfrac{\partial}{\partial z}\left(\dfrac{1}{m(z)}\dfrac{\partial \Psi_n^{(l+1)}(z)}{\partial z}\right) + V^{(l+1)}(z)\Psi_n^{(l+1)}(z) = E_n^{(l+1)}\Psi_n^{(l+1)}(z), \\ \dfrac{\partial}{\partial z}\left(\varepsilon(z)\dfrac{\partial \varphi_{\rm H}^{(l)}(z)}{\partial z}\right) = -e\rho^{(l)}(z) \end{cases}, \tag{34}$$

where the effective potential in the first order of iterations is considered to be equal:

$$V^{(1)}(z) = \Delta E_C(z) + V_{\rm E}(z). \tag{35}$$

The accuracy of the calculations performed according to the scheme (34) is given by the following conditions:

$$\begin{gathered} \dfrac{\left|\left|\Psi_n^{(l+1)}(z)\right|^2 - \left|\Psi_n^{(l)}(z)\right|^2\right|}{\left|\Psi_n^{(l)}(z)\right|^2} \ll 1; \\ \dfrac{\left|\varphi_{\rm H}^{(l)}(z) - \varphi_{\rm H}^{(l-1)}(z)\right|}{\varphi_{\rm H}^{(l)}(z)} \ll 1. \end{gathered} \tag{36}$$

V. DISCUSSION OF THE RESULTS

The calculation of the effective potential $V(z)$, the stationary energy spectrum of the electron E_n , its wave functions $\Psi_n(E_n, z)$, and the oscillator strengths of quantum transitions $f_{m,m'}$ were performed on the basis of the developed theory.

Calculations were performed for the experimentally implemented nanostructure being a separate QCD cascade [5]. The geometric parameters of RTS were as follows: the thickness of potential barriers: $\Delta_1 = 2$ nm; $\Delta_2 = 1$ nm; $\Delta_3 = 1$ nm, the width of the potential wells: $d_1 = 2.08$ nm; $d_2 = 15$ nm.

The pysical parameters of the RTS material layers: $a\,(nm)$; m/m_0; ε; $P_{\rm SP}(C/m^2)$; $e_{31}\ (C/m^2)$, $e_{33}\ (C/m^2)$; $c_{11}(GPa)$, $c_{12}(GPa)$, $c_{13}(GPa)$, $c_{33}(GPa)$ are known from the literature [27, 29], their values are given in Table 1, where m_0 ia the mass of a free electron.

	a	m/m_0	ε	$P_{\rm SP}$	e_{31}	e_{33}	c_{11}	c_{12}	c_{13}	c_{33}
AlN	0.31106	0.322	8.5	−0.081	−0.53	1.51	396	137	108	373
GaN	0.31892	0.186	10	−0.034	−0.34	0.67	390	145	106	398
$Al_{0.58}Ga_{0.42}N$	0.31436	0.265	9.13	−0.061	−0.45	1.15	393.5	140.4	107.2	383.5

Table 1. Physical parameters of the RTS material layers.

The concentration of donor impurities according to experimental work [5] was chosen equal to $N_{\rm D} = 6 \times 10^{17}$ cm^{-3}, temperature was $T = 273$ K.

The accuracy of the calculations, which is given by the relations (36), was assumed to be equal to 10^{-6}, which was insured by 8–10 iterations according to the scheme (34).

In Fig. 2 the energetic scheme of a single QCD cascade is presented, the calculation of the potential profile of which, depending on the value of z, was performed according to the relations (3), (8), (11), (12). It can be seen from the figure that in comparison with the QCD cascades operating in the middle and far infrared ranges [7, 8], the depths of potential wells and the height of potential barriers are much larger and significantly deformed under the influence of internal electric fields caused by spontaneous and piezoelectric polarizations. It should be noted that this fact is promising for varying the performance characteristics of nanoscale devices by changing the parameters of the geometric design of the RTS cascade [30–32].

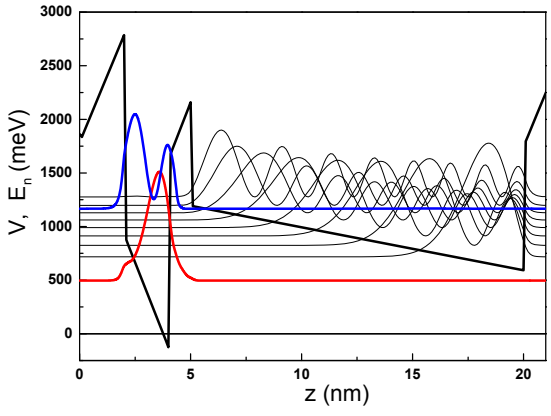

Fig. 2. Potential profile of one cascade of QCD and square moduli of the stationary states wave functions.

In Fig. 2 the values of the energies of the stationary electron spectrum in the investigated RTS and the corresponding distributions of the probability of finding an electron within the nanosystem $|\Psi(E_n, z)|^2$ are presented. The values of these energies and the localization of their corresponding electronic states in the RTS are presented in Table 2. It can be seen from the figure that the operating electron states, which are localized in the RTS input well, cause a vertical electronic transition $1 \to 8$ with energy $\Omega^{(\text{theory})} = E_8 - E_1 = 660.3\,\text{meV}$. The calculated value of the detected energy differs from the experimentally obtained value $\Omega^{(\text{exp})} = 650.0\,\text{meV}$ by not more than 2%.

Electron energy (meV)	Localization
E_1=496.6	active band
E_2=686.6	extractor
E_3=793.9	extractor
E_4=881.7	extractor
E_5=959.3	extractor
E_6=1030.3	extractor
E_7=1097.6	extractor
E_8=1156.8	active band
E_9=1245.3	extractor
E_{10}=1336.0	extractor

Table 2. The values of the stationary spectrum energies of an electron in the closed RTS and their localization.

Next, we calculated the energy of the stationary electron spectrum (E_n) and the oscillator forces of quantum transitions ($f_{nn'}$). The results are presented in Fig. 3a,b, depending on the position d ($0 \le d \le d_1 + d_2$) of the inner barrier between the two outer barriers of RTS, the sizes of all its other its elements being fixed. It can be seen from Fig. 3,a, that for each energy level number n the dependence $E_n = E_n(d)$ forms n maxima and $n-1$ minima, respectively. In this case, the condition $E_n(d)|_{d\to 0} \approx E_n(b)|_{d\to d_1+d_2}$, that holds for active zones of the arsenide semiconductors QCD and QCL is not satisfied. The new condition looks like:

$$E_n(d)|_{d\to 0} \approx E_n(d)|_{d\to d_1+d_2} + V_{\text{H}}(d_1+d_2) + V_{\text{ex}}(d_1+d_2) + V_{\text{E}}(d_1+d_2). \quad (37)$$

The condition that determines the optimal operation of the QCD is the formation of the maximum value of the oscillator strength $f_{nn'}$ of the quantum transition between electronic states, providing the necessary energy of the electromagnetic field absorbing??? [30, 32] (in our case this is $\Omega_{18} = E_8 - E_1$). Thus, it is necessary for the oscillator strength f_{18} to be in order of magnitude larger than the oscillator strength of the quantum transitions from the first to the remaining stationary electronic states, that is:

$$f_{18} \gg f_{1n'},\ n' = \overline{2\ldots 9},\ n' \neq 8. \quad (38)$$

The results of calculating the oscillator strengths of quantum transitions from the first electronic stationary state to the rest electronic states contained in the RTS as a function of the value of d are shown in Fig. 3,b. It is clear from the figure that the necessary condition (34) is satisfied by a single region 1.7 nm $\le d \le$ 2.8 nm containing the experimentally realized configuration of the QCD active band d_{exp}.

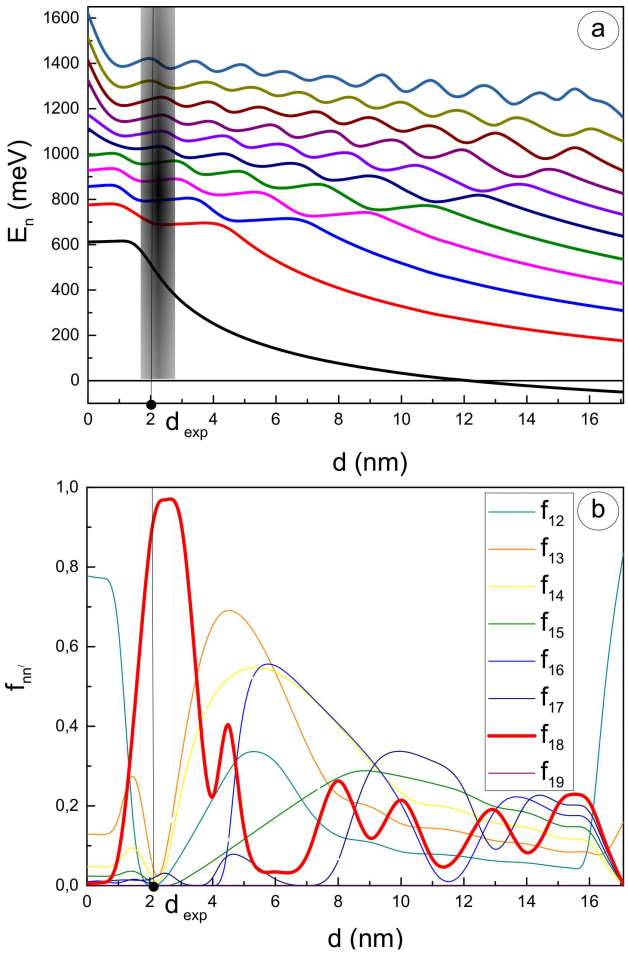

Fig. 3. Electron stationary spectrum (a), oscillator strengths (b) as functions of the position (d) of the inner barrier between the two outer barriers of RTS.

Thus, the developed theory allows to establish geometric configurations of nitride QCD active zones, which ensure optimal operation of these nanodevices.

VI. CONCLUSIONS

1. Using the solutions to the self-consistent system of the Schrödinger and Poisson equations the theory of stationary electronic states and the forces of oscillators of quantum transitions in an anisotropic RTS of wurtzite type has been developed.

2. For the experimentally produced QCD of the near-infrared range, the calculation of effective potential,

stationary electron spectrum and forces of oscillator strengths of quantum transitions has been performed.

3. It is shown that the calculated value of the detected energy differs from the experimentally obtained by no more than 2%. It is established that in the vicinity of an experimentally realised configuration of the nanostructure the intensity of quantum transitions between the working electron states determining the operating value of detected energy is maximal.

4. The proposed theory can be used for the calculation of the potential profiles of wurtzite anisotropic RTS, spectral parameters of an electron and to determine the geometric configurations of these nanostructures, which provide the optimal operation of nanodevices on their basis.

VII. ACKNOWLEDGEMENTS

The author is sincerely grateful to Head of the Chair of Theoretical Physics and Computer Modelling of Yu. Fed'kovych National University of Chernivtsi, Dr. Sci., Professor M. V. Tkach for his useful advice concerning the writing of this work and the discussion of the results obtained. This work was partially performed under the project 0117U001151 with the financial support of Ministry of Education and Science of Ukraine.

[1] W. Terashima, H. Hiray, Phys. Status Solidi C **S2**, 615 (2009).
[2] B. Mirzaei, A. Rostami, H.Baghban, Opt. Laser Technol. **44**, 378 (2012).
[3] D. Hofstetter, J. D. Francesco, P. K. Kandaswamy, E. Monroy, Appl. Phys. Lett. **98**, 071104 (2011).
[4] S. Sakr, E. Giraud, A. Dussaigne, M. Tchernycheva, N. Grandjean, F. H. Julien, Appl. Phys. Lett. **100**, 181103 (2012).
[5] S. Sakr *et al.*, Appl. Phys. Lett. **101**, 251101 (2012).
[6] A. Lyakh, M. Suttinger, R. Go, P. Figueiredo, A. Todi, Appl. Phys. Lett. **109**, 121109 (2016).
[7] D. Turcinkova *et al.*, Appl. Phys. Lett. **99**, 191104 (2011).
[8] P. Reininger *et al.*, Appl. Phys. Lett. **103**, 241103 (2013).
[9] P. Reininger *et al.*, Appl. Phys. Lett. **105**, 091108 (2014).
[10] F. Bernardini, V. Fiorentini, D. Vanderbilt, Phys. Rev. B **56**, R10024 (1997).
[11] F. Bernardini, V. Fiorentini, Phys. Rev. B **57**, R9427 (1998).
[12] F. Bernardini, V. Fiorentini, Phys. Status Solidi B **216**, 391 (1999).
[13] A. Zoroddu, F. Bernardini, P. Ruggerone, V. Fiorentini, Phys. Rev. B **64**, 045208 (2001).
[14] O. Ambacher *et al.*, J. Phys.: Condens. Matter **14**, 3399 (2002).
[15] F. Bernardini, V. Fiorentini, Phys. Rev. B **64**, 085207 (2002).
[16] B. K. Ridley, W. J. Schaff, L. F. Eastman, J. Appl. Phys. **94**, 3972 (2003).
[17] J. Radovanović, V. Milanović, J. Appl. Phys. **92**, 7672 (2002).
[18] J. Radovanović *et al.*, IEEE J. Quantum Electron. **39**, 1297 (2003).
[19] J.M. Lia *et al.*, J. Vac. Sci. Technol. **39**, 2568 (2004).
[20] I. Supryadkina, K. Abgaryan, D. Bazhanov, I. Mutigullin, Phys. Status Solidi C **11**, 307 (2014).
[21] K. Abgaryan, I. Mutigullin, D. Reviznikov, Phys. Status Solidi C **12**, 460 (2015).
[22] Z. Gu, S. L. Ban, J. Appl. Phys. **110**, 013722 (2011).
[23] Z. Gu, S. L. Ban, D. D. Jiang, Y. Qu, J. Appl. Phys. **121**, 035703 (2017).
[24] N. Nepal, J. Li, M. L. Nakarmi, J. Y. Lin, H. X. Jiang, Appl. Phys. Lett. **87**, 242104 (2005).
[25] I. Vurgaftman, J. R. Meyer, J. Appl. Phys. **94**, 3675 (2003).
[26] L. Hedin, B.I. Lundqvist, J. Phys. C **4**, 2064 (1971).
[27] F. Bernardini, V. Fiorentini, D. Vanderbilt, Phys. Rev. B **63**, 193201 (2002).
[28] A.A. Samarskii, *The Theory of Difference Schemes*, (Marcel Dekker, New York, 2001).
[29] P. K. Kandaswamy *et al.*, J. Appl. Phys. **104**, 093501 (2008).
[30] M. V. Tkach, Ju. O. Seti, I. V. Boyko, O. M. Voitsekhivska, Condens. Matter Phys. **16**, 33701 (2013).
[31] I. V. Boyko, Ukr. J. Phys. **61**, 66 (2016).
[32] M. V. Tkach, Ju. O. Seti, V. O. Matijek, I. V. Boyko, J. Phys. Stud. **16**, 4701 (2012).

АНІЗОТРОПНІ ВЮРЦИТНІ РЕЗОНАНСНО-ТУНЕЛЬНІ СТРУКТУРИ: СТАЦІОНАРНИЙ СПЕКТР ЕЛЕКТРОНА ТА СИЛИ ОСЦИЛЯТОРІВ КВАНТОВИХ ПЕРЕХОДІВ

І. В. Бойко
Тернопільський національний технічний університет імені Івана Пулюя,
вул. Руська, 56, Тернопіль, 46001, Україна
e-mail: boyko.i.v.theory@gmail.com

З використанням моделі діелектричного континууму та моделі ефективних мас для електрона знайдено самоузгоджені розв'язки системи рівнянь Шредингґера–Пуассона з урахуванням внеску п'єзоелектричної та спонтанної поляризацій.

Для трибар'єрної анізотропної резонансно-тунельної структури вюрцитного типу з подвійними та потрійними компонентами розвинено теорію стаціонарних електронних станів, що враховує вплив внутрішніх полів, зумовлених п'єзоелектричною та спонтанною поляризаціями, які виникають у наноструктурі.

Для наноструктури, що функціонувала як каскад експериментально реалізованого квантового каскадного детектора, виконано розрахунок потенціального профілю, стаціонарного енергґетичного спектра електрона та сил осциляторів квантових переходів. Установлено геометричні конфіґурації наноструктури, для яких інтенсивність квантових детекторних переходів між робочими енергґетичними станами найбільша.